HHS Public Access

Author manuscript

*FASEB J.* Author manuscript; available in PMC 2021 April 01.

Published in final edited form as:

*FASEB J.* 2020 April ; 34(4): 5642–5657. doi:10.1096/fj.201902105R.

# *Abcg2*-Expressing Side Population Cells Contribute to Cardiomyocyte Renewal through Fusion

**Amritha Yellamilli**[1,2,3], **Yi Ren**[1], **Ron T. McElmurry**[3,4], **Jonathan P. Lambert**[5], **Polina Gross**[6], **Sadia Mohsin**[6], **Steven R. Houser**[6], **John W. Elrod**[5], **Jakub Tolar**[3,4], **Daniel J. Garry**[1], **Jop H. van Berlo**[1,2,3]

[1.]Lillehei Heart Institute, Department of Medicine, University of Minnesota, Minneapolis, MN USA

[2.]Department of Integrative Biology and Physiology, University of Minnesota, Minneapolis, MN USA

[3.]Stem Cell Institute, University of Minnesota, Minneapolis, MN USA

[4.]Department of Pediatrics, University of Minnesota, Minneapolis, MN USA

[5.]Center for Translational Medicine, Lewis Katz School of Medicine at Temple University, Philadelphia, PA USA

[6.]Cardiovascular Research Center, Lewis Katz School of Medicine at Temple University, Philadelphia, PA USA

## Abstract

The adult mammalian heart has a limited regenerative capacity. Therefore, identification of endogenous cells and mechanisms that contribute to cardiac regeneration is essential for the development of targeted therapies. The side population (SP) phenotype has been used to enrich for stem cells throughout the body; however, SP cells isolated from the heart have been studied exclusively in cell culture or after transplantation, limiting our understanding of their function *in vivo*. We generated a new *Abcg2*-driven lineage-tracing mouse model with efficient labeling of SP cells. Labeled SP cells give rise to terminally differentiated cells in bone marrow and intestines. In the heart, labeled SP cells give rise to lineage-traced cardiomyocytes under homeostatic conditions with an increase in this contribution following cardiac injury. Instead of differentiating into cardiomyocytes like proposed cardiac progenitor cells, cardiac SP cells fuse with preexisting cardiomyocytes to stimulate cardiomyocyte cell cycle reentry. Our study is the first to show that fusion between cardiomyocytes and non-cardiomyocytes, identified by the SP phenotype, contribute to endogenous cardiac regeneration by triggering cardiomyocyte cell cycle reentry in the adult mammalian heart.

**Correspondence:** Jop H. van Berlo, M.D., Ph.D., Lillehei Heart Institute, 2231 6th St SE, Minneapolis, MN 55455, Office: (612) 626-1853, jvanberl@umn.edu.

AUTHOR CONTRIBUTIONS

A.Yellamilli and J.H.van Berlo designed research, analyzed data, and wrote paper. A.Yellamilli performed research for all studies. Y. Ren analyzed MoFlo flow cytometry data. R.T. McElmurry and J. Tolar generated bone marrow chimeric mice. J.P. Lambert, P. Gross, S. Mohsin, S.R. Houser, and J.W. Elrod performed $Ca^{2+}$ transient and fractional shortening experiments. D.J. Garry assisted with data interpretation and edited the manuscript.

**Keywords**

Cardiac Regeneration; Side Population; Fusion; Cardiomyocyte Proliferation

## INTRODUCTION

A critical feature of heart failure that limits the effectiveness of current therapies is loss of functional cardiomyocytes(1, 2). Since the adult heart has a limited ability to generate new cardiomyocytes, strategies that increase the number of cardiomyocytes in failing hearts are actively being developed(3, 4). To date, the main strategy studied in patients with ischemic heart disease or heart failure has been transplantation of bone-marrow-derived cells or proposed cardiac progenitor cells. Originally, it was postulated that transplanted cells engrafted and differentiated into cardiomyocytes; however, it is now widely accepted that these cells are not retained in the heart and any beneficial effect reported is due to paracrine effects on endogenous cells. Moreover, scientific studies that formed the foundation of these clinical trials have been called into question with several studies being retracted in recent years(5). Because of this, the field of cardiac regeneration has shifted its focus away from transplantation of proposed progenitor cells as a direct source of new cardiomyocytes(6-11).

A growing area of interest is understanding the regenerative potential of endogenous cells in the heart using *in vivo* approaches. Currently, proliferation of preexisting cardiomyocytes is believed to be the sole source of new cardiomyocytes(12, 13) and recent publications have questioned the existence of any progenitor cell population with the ability to differentiate into cardiomyocytes in the adult heart(14-16). To assess whether endogenous cardiac progenitor cells exist in an unbiased manner without using previously studied membrane markers, we utilized the side population phenotype that enriches for stem cells throughout the body and in different forms of cancer(17-20). The side population phenotype is the ability of cells to extrude Hoechst 33342, a fluorescent DNA dye, out of their cytoplasm. To identify side population cells (SPCs), a single cell suspension is incubated with Hoechst 33342 and analyzed with flow cytometry to identify cells that extrude Hoechst 33342, thereby sorting to the “side” of the main population of cells(21). The side population phenotype was first described as a way to enrich for hematopoietic stem cells (HSCs) capable of long-term bone marrow reconstitution after transplantation into lethally irradiated mice(21). Since then, SPCs have been identified in many organs including intestines, skeletal muscle, and heart(22).

Isolated cardiac side population cells (cSPCs) are enriched for cells that self-renew and differentiate into multiple cardiac lineages in cell culture and after transplantation(20, 22-24). Cultured cSPCs form colonies at ten times the rate of other non-cardiomyocytes isolated from the heart(19, 25). Primary and secondary cSPC clones can be maintained in cell culture for over ten months with preservation of the side population phenotype and without undergoing replicative senescence(24). In cell culture and transplantation studies, cSPCs are also multipotent. They differentiate towards cardiomyocyte, endothelial cell, or smooth muscle cell lineages under specific culture conditions(22). In preclinical studies, transplanted cSPCs engraft in the heart after cryoinjury or myocardial ischemia (MI) and

give rise to cardiomyocytes, endothelial cells, smooth muscle cells, and fibroblasts(23, 24, 26). Importantly, cSPCs are a distinct population of cells from cardiac *Kit*-expressing cells – they do not express *Kit* and have a completely unique expression pattern from cardiac *Kit*-expressing cells(24, 25, 27).

Since studies of cSPCs have been limited to cell culture and transplantation, it is not known whether the side population phenotype can be used to identify endogenous cardiac progenitor cells that gives rise to cardiomyocytes *in vivo*. Here, we studied the role of endogenous cSPCs in cardiac regeneration using a newly-generated, lineage-tracing mouse model driven by the *Abcg2* gene that encodes a transporter essential for the side population phenotype(19, 28-31).

## MATERIALS AND METHODS

### Experimental Mouse Models.

All animal procedures were performed conforming to the NIH guidelines and approved by the University of Minnesota Institutional Animal Care and Use Committee. No human subjects or human materials were used. Standard gene targeting of the murine *Abcg2* locus was done to insert a complementary DNA encoding Cre recombinase flanked by a mutated estrogen receptor. A targeting vector containing ampicillin resistance and a diphtheria toxin A cassette was used to insert homology arms upstream and downstream of the ATG start codon containing second exon of *Abcg2*, the cDNA for MerCreMer cloned in-frame with the ATG start codon of *Abcg2*, as well as a frt site flanked neomycin selection cassette through recombineering. A linearized targeting vector was electroporated into embryonic stem (ES) cells and correctly targeted clones were identified by PCR and Southern blot analysis. ES cell aggregation with 8-cell embryos was used to generate chimeric mice. Germline transmitting chimeras were cross-bred with Rosa26-Flpe mice (B6.129S4-Gt(ROSA)26Sortm1(FLP1)Dym/RainJ) to delete the neomycin selection cassette. We generated experimental animals by cross-breeding Abcg2$^{MCM/+}$ mice to previously modified FVB.Cg-Gt(ROSA)26Sor$^{tm1(CAG-lacZ,EGFP)Glh}$/J (11), B6.129(Cg)-Gt(ROSA)26Sor$^{tm4(ACTB-tdTomato,-EGFP)Luo}$/J, B6;129S6-Gt(ROSA)26Sor$^{tm1(CAG-tdTomato*,-EGFP*)Ees}$/J, or B6.Cg-*Gt(ROSA)26Sor$^{tm14(CAG-tdTomato)Hze}$*/J mice (all reporter mice were purchased from the Jackson Laboratory). A previously published BAC transgenic Cdh5 CreERT2 mouse line was cross-bred to R26$^{GFP/GFP}$ mice(32). A previously published Myosin Heavy Chain 7Cre mouse line was cross-bred to B6.Cg-*Gt(ROSA)26Sor$^{tm14(CAG-tdTomato)Hze}$*/J mice(33). PCR genotyping of Abcg2$^{MCM/+}$ was performed with the following primers: wild type fw: 5'-tcaaagtgctggtatctgtgttga-3', wild type rev: 5'-catgaattgaagtatccacagcaa-3', mut fw: 5'-ggtgggacatttgagttgct-3', mut rev: 5'-catatgtacaacaacatgaattgaagtatcc-3', MerCreMer fw: 5'-ggcgttttctgagcatacct-3', MerCreMer rev: 5'-ctacaccagagacggaaatcc-3'. Previously published *Abcg2* knockout mice were used to verify antibody specificity(30). Both males and female mice were used in all experiments.

### Chemicals.

To induce Cre-mediated recombination, 8-week-old mice were injected intraperitoneally with 2 mg of tamoxifen for 5 consecutive days. DNA synthesis was measured by labeling with 5-Ethynyl-2'-deoxyuridine (EdU). The timing and frequency of intraperitoneal injections is shown in the experimental schematics, where every arrow indicates one intraperitoneal injection of 2.5 mg of EdU. For isoproterenol studies, mice were given subcutaneous 100 mg/kg injections into the loose skin overlying their scapulae once a day, for five consecutive days starting 72 hours after the final tamoxifen injection was given. Vehicle control mice were subcutaneously injected with a similar volume 0.9% sodium chloride solution.

### Myocardial ischemia (MI) surgery.

Seventy-two hours after the final tamoxifen injection, mice were anesthetized with 3% isoflurane, intubated via intratracheal intubation and maintained on 2.5% isoflurane throughout the surgery. A parasternal thoracotomy was performed, followed by permanent ligation of the left coronary artery just below the left atrial auricle using 7–0 silk suture(34). After confirming ligation by visual observation of myocardial blanching distal to the suture; the musculature and skin were sequentially closed in layers and mice were allowed to recover on a heating pad. For sham-operated mice, the same steps were completed except for ligation of the left coronary artery. Mice were given subcutaneous buprenorphine SR-LAB prior to the start of surgery. Aseptic technique was used for all surgical procedures.

### Isolation and FACS analysis of bone marrow side population cells and lineages.

Bone marrow cells were isolated and analyzed for side population phenotype and presence of lineage markers using published protocols(35). Bone marrow was isolated from bilateral femora and tibiae. For side population analysis, bone marrow cells were incubated with 5 μg/mL Hoechst 33342 for 90 minutes in a 37°C water bath. As a negative control, bone marrow cells were incubated with both 5 μg/mL Hoechst 33342 and 50 μM verapamil under the same conditions. Hoechst 33342-stained cells were subsequently stained with a biotinylated lineage antibody panel followed by staining with streptavidin conjugated to Alexa Fluor™ 647, α-Sca-1 PE antibody and α-Kit APC antibody for $Lineage^{-}Sca\text{-}1^{+}Kit^{+}$ (LSK) analysis. For bone marrow lineages, freshly isolated bone marrow cells were stained with either α-CD3ε biotin, α-CD11b biotin, α-CD45R biotin, α-Ly6G and Ly6C biotin or α-Ter119 biotin followed by streptavidin conjugated to Alexa Fluor 647. Before FACS analysis, propidium iodide was added to all samples at a final concentration of 2 μg/mL for live cell/dead cell discrimination. Bone marrow side population cell data were acquired using the MoFlo XDP flow cytometer cell sorter and analyzed using the accompanying Summit™ software.

### Bone marrow transplantation.

Transgenic Myosin Heavy Chain 7 $^{Cre/+}$ mice cross-bred with $R26^{Tomato/+}$ mice were conditioned with 11.0 Gy total body irradiation one day before transplantation. Bone marrow was isolated from $Abcg2^{MCM/+}$ $R26^{GFP/+}$ mice that had not received tamoxifen injections. HSCs were enriched using the EasySep Mouse Hematopoietic Progenitor Cell

Enrichment kit (Stemcell Technologies, Seattle, WA) and $1*10^6$ HSCs were administered via tail vein injection to recipient mice. Ten weeks after transplantation, bone marrow chimeric mice were intraperitoneally injected with 2 mg tamoxifen for 5 consecutive days. Four weeks after the final tamoxifen injection, GFP-labeling of bone marrow side population cells, bone marrow differentiated lineages, and cardiomyocytes from histological sections were analyzed.

### Isolation and FACS analysis of cardiac side population cells and non-cardiomyocyte lineages.

Non-cardiomyocytes were isolated from the heart and analyzed for the side population phenotype and differentiated lineage markers using a previously published protocol(36). Hearts were flushed with ice-cold PBS to remove red blood cells, minced into a fine slurry and digested in a solution containing 2.4 U/mL Dispase II, 0.1% Collagenase B, and 2.5 mM calcium chloride for 30 minutes in a 37°C water bath. Next, the digestion solution was triturated, strained through a 70 μm cell strainer followed by a 40 μm cell strainer, and centrifuged at 600 g for 5 minutes at 4°C to pellet non-cardiomyocytes out of the digestion solution. For cardiac side population analysis, non-cardiomyocytes were stained with 1.5 μg/mL Hoechst 33342 for 90 minutes in a 37°C water bath. As a negative control, non-cardiomyocytes were also stained with 1.5 μg/mL Hoechst 33342 and 50 μM verapamil under the same conditions. For non-cardiomyocyte lineages, freshly isolated non-cardiomyocytes were stained with either α-CD45 PE or α-CD31 APC. Before FACS analysis, propidium iodide was added to all samples at a final concentration of 2 μg/mL for live cell/dead cell discrimination. Cardiac side population cell data were acquired using a MoFlo™ XDP flow cytometer cell sorter and analyzed using the accompanying Summit software. Non-cardiomyocyte lineage data were acquired using a BD FACSAria II flow cytometer cell sorter and analyzed using FlowJo v10 software application.

### Tissue processing for histology.

All tissues for histology were fixed with 4% paraformaldehyde for 3 hours at room temperature with gentle rocking, washed with PBS, and incubated in a 30% sucrose solution (w/v in PBS) overnight at 4°C. After tissues sunk down to the bottom of specimen tubes, they were trimmed, embedded in O.C.T. and frozen over a slurry of dry ice and isopentane. Hearts were cut and embedded in a four-chamber orientation. Blocks were cut into 5 μm sections and were mounted onto Fisherbrand Superfrost Plus Microscope slides. Blocks and slides were stored at −80˚C until further use.

### Histological stains, image acquisition and analysis.

To identify non-cardiomyocytes and cardiomyocytes on histological sections, cryosections were stained with primary antibodies. Briefly, slides were air-dried for 5 minutes, washed with 0.1% Triton X-100 (v/v in PBS), blocked for 1 hour at room temperature in antibody-specific blocking solution, and incubated with primary antibodies overnight at 4°C. The following day, slides were washed, incubated with secondary antibodies and DAPI and washed before coverslips were mounted on the slides using Vectashield mounting medium. Antibodies used include Abcg2 (BXP-53 Santa-Cruz, rat monoclonal 1:400), CD31 (Lifespan Biosciences LS-B4737, rabbit polyclonal 1:20), Vimentin (Abcam ab45939, rabbit

polyclonal 1:50), CD45 (R&D Systems, goat polyclonal 1:20), α-SMA (Abcam ab5694, rabbit polyclonal 1:150), Lyve1 (Abcam ab14917, rabbit polyclonal 1:250), NG2 (Millipore AB5320, rabbit polyclonal 1:150), Troponin I (Abcam ab47003, rabbit polyclonal 1:100). For EdU staining, the Click-iT Plus EdU Alexa Fluor Imaging Kit was used and nuclei were counter stained with DAPI. All immunohistochemically stained slides were imaged using a Zeiss Axio Imager M1 Upright Microscope.

To quantify GFP-labeling of cardiomyocytes on histological sections, cryosections were stained with Wheat Germ Agglutinin conjugated to Texas Red-X and DAPI. Ten separate images were taken with a 20X objective throughout the left ventricle using the Zeiss Axio Imager M1 Upright Microscope. The number of GFP-labeled cardiomyocytes was counted for each field-of-view and quantification of GFP-labeled cardiomyocytes was calculated as the percent of GFP-labeled cardiomyocytes out of total cardiomyocytes.

For Sirius Red/ Fast Green staining, cryosection slides were fixed with pre-warmed Bouin's fixative at 55°C for 1 hour, stained with 0.4% Fast Green (v/v in picric acid) for 10 minutes at room temperature followed by 0.1% Sirius Red (v/v in picric acid) for 30 minutes at room temperature. After each stain, slides were washed with running tap water to remove excess dye. Coverslips were mounted with Permount Mounting Medium. Slides were then imaged using a Huron Technologies TISSUEscope LE brightfield slide scanner available at the University Imaging Center at the University of Minnesota. Slide images were viewed using the free HuronViewer software. Frozen sections from $Abcg2^{MCM/+}$ $R26^{mTmG/+}$ were stained with DAPI and imaged using a Nikon C2 and Nikon A1 confocal microscope at the University Imaging Centers, University of Minnesota.

### Isolation and analysis of adult cardiomyocyte.

Adult cardiomyocytes were isolated using a previously published protocol(37). After excision, hearts were cannulated on a gravity-dependent Langendorff perfusion setup and perfused with 2.4 mg/mL Collagenase type 2 solution for 9–11 minutes. Digested hearts were cut into 10–12 pieces and gentle triturated to release individual cardiomyocytes. Cardiomyocytes were pelleted by centrifuging digestion solution at 19 g for 5 minutes. The total numbers of rod-shaped and rounded-up cardiomyocytes were counted using a Fuchs-Rosenthal counting chamber. The number of GFP-labeled rod-shaped cardiomyocytes was counted by an individual blinded to the experimental conditions using a Zeiss Axio Observer Z1 Inverted Microscope. Quantification of GFP-labeled cardiomyocytes was calculated as the percent of total rod-shaped cardiomyocytes labeled with GFP.

For Troponin T and EdU staining, isolated adult cardiomyocytes were immediately fixed with 4% paraformaldehyde (v/v in PBS) for 5 minutes followed by washing with PBS before EdU and Troponin T staining. For Troponin T staining, cardiomyocytes were washed with 0.1% Triton X-100 (v/v in PBS), blocked for an hour at room temperature with 5% normal goat serum (v/v in PBS), and incubated with Troponin T antibody (Thermo Fisher MS295, mouse monoclonal 1:100) overnight at 4°C. The following day, cardiomyocytes were washed and incubated with Donkey α-mouse antibody Alexa Fluor 568 and DAPI (50 ng/mL). EdU-stained cardiomyocytes were also stained for GFP (Abcam ab290, rabbit polyclonal 1:100) using the same protocol outlined for Troponin T staining. All data from

isolated adult cardiomyocytes was acquired using a Zeiss Axio Observer Z1 Inverted Microscope.

### qPCR on isolated adult cardiomyocytes and endothelial cells.

Adult cardiomyocytes and endothelial cells were isolated by individually digesting the hearts of 6 mice using retrograde perfusion (see above). After complete digestion of the heart, the tissue was teased apart and filtered through 200μm mesh. Isolated cells were differentially centrifuged at 100G, where the pellet was enriched for cardiomyocytes while the supernatant was further processed for endothelial cell enrichment. Endothelial cell enrichment was performed using CD31 microbeads and MACS columns. RNA was isolated from cardiomyocytes and endothelial cells using the Norgen RNA purification kit according to the manufacturer's instructions and following previously published methods(38). RNA concentration was measured using a Nanodrop, and normalized input RNA was used to generate cDNA using a Superscript VILO cDNA synthesis kit (Invitrogen). Expression of *Abcg2* and *Pecam1* was determined by quantitative PCR using Taqman primers and probes on a 7900HT Fast Real-Time PCR system. Relative expression was normalized to GAPDH based on the 2(-ΔΔ C(t)) method.

### Adult Cardiomyocyte cytosolic calcium ($_cCa^{2+}$) transient recordings.

Isolated adult cardiomyocytes were loaded with 1 μM Fluo-4 AM and placed in a 37°C chamber on an inverted microscope stage (Zeiss Axio Observer Z1, Sutter DG4 plus: excitation, and Sutter Lambda 10–2: emission and images are acquired using a Photometrics Evolve Delta EMCCD camera) as previously detailed(39). Adult cardiomyocytes were perfused with a physiological Tyrode's buffer (150 mM NaCl, 5.4 mM KCl, 1.2 mM $MgCl_2$, 10 mM glucose, 2 mM sodium pyruvate, and 5 mM HEPES, pH 7.4) containing 2 mM $CaCl_2$. Cells were paced at 1 Hz and $_cCa^{2+}$ transients continuously recorded and analyzed offline with pCLAMP 10 software. After two minutes of baseline recording, 100 nM isoproterenol was applied by changing the perfusion solution. For $_cCa^{2+}$ fluorescence measurements, background fluorescence was subtracted and changes in $[Ca^{2+}]$ are expressed as changes of normalized fluorescence, F/F0, where F denotes the maximal fluorescence (peak) and F0 (or F unstimulated), is the resting fluorescence at the beginning of each recording (average fluorescence of the cell 50 ms prior to stimulation). For fractional shortening measurements, isolated adult cardiomyocytes were placed in a heated chamber (37°C) on the stage of an inverted microscope and perfused with a normal physiological Tyrode's buffer 2 mM $CaCl_2$ and paced by field-stimulation at 1 Hz (100 ms pulse duration). Fractional shortening measurements were taken from both ends of each cell using a video edge detection system (Crescent Electronics, Sandy, UT) and after two minutes of baseline recording, 100 nM isoproterenol was applied by changing the perfusion solution. All data is paired, i.e. all baseline %FS values have accompanying values post-iso treatment.

### Statistical Analysis.

Results are reported as mean ± standard deviation. For adult cardiomyocyte cytosolic calcium transient recordings and fractional shortening measurements data are reported as mean ± standard error of the mean. Student's t-tests were performed to compare two groups

and 2-way ANOVA to compare multiple groups. p-values less than 0.05 were considered statistically significant.

## RESULTS

### Lineage-tracing mouse model reliably and specifically labels *Abcg2*-expressing cells.

To lineage-trace endogenous SPCs, we generated an *Abcg2*-driven lineage-tracing mouse model in which cDNA encoding a tamoxifen-inducible MerCreMer (MCM) fusion protein was inserted into the endogenous *Abcg2* locus (Abcg2$^{MCM/+}$). These mice were cross-bred with Cre-inducible reporter mice, R26$^{GFP/GFP}$, to generate experimental Abcg2$^{MCM/+}$ R26$^{GFP/+}$ mice (Figure 1A). Two different tamoxifen injection strategies were used to induce recombination (Figures 1B and 1C). With this approach, we first verified that *Abcg2*-expressing cells were specifically labeled in Abcg2$^{MCM/+}$ R26$^{GFP/+}$ mice injected with tamoxifen. ABCG2 is expressed at the apical surfaces of renal proximal tubules and intestinal epithelium, on canalicular membranes of hepatocytes, and by cardiac endothelium(40-42). We confirmed this reported expression pattern with immunofluorescent staining using an ABCG2-specific antibody on renal, ileal, hepatic, and cardiac histological sections from wild type mice (Figure 1D). No staining was observed on sections from *Abcg2*-knockout mice(30), confirming specificity of the antibody used (Figure S1A). To determine whether the *Abcg2*-driven lineage-tracing mouse model accurately labels *Abcg2*-expressing cells, we imaged native fluorescence of GFP in tissues harvested from tamoxifen-injected Abgc2$^{MCM/+}$ R26$^{GFP/+}$ mice at week 9 (Figure 1B). We observed extensive labeling of cells in the kidney, ileum, liver, and heart known to express ABCG2 (Figure 1E). Notably, no GFP-labeling was observed in vehicle-injected Abgc2$^{MCM/+}$ R26$^{GFP/+}$ mice, indicating no aberrant translocation of MCM into the nucleus without tamoxifen induction (Figure S1B). GFP-labeling in all other organs appeared to be restricted to endothelial cells (Figure S1C).

### Bone marrow and intestinal SPCs are enriched for endogenous stem cells that give rise to terminally differentiated cells *in vivo*.

Next, we lineage-traced bone marrow SPCs to determine whether they enrich for endogenous hematopoietic stem cells(21). Bone marrow SPCs were accurately identified with flow cytometry using negative control samples incubated with Verapamil, a non-specific ABC-transporter inhibitor that blocks the side population phenotype (Figures 1F and 1G). In bone marrow of Abgc2$^{MCM/+}$ R26$^{GFP/+}$ mice injected with tamoxifen, 66.2 ± 18.4% of SPCs (Figure 1H, n=6) and 65.7 ± 16.8% (n=5) LSK (Lineage marker$^{-}$, Sca-1$^{+}$, Kit$^{+}$) HSCs were labeled with GFP. Moreover, 92.6 ± 8.5% (n=3) of LSK cells within the side population gate were GFP-labeled. To evaluate the contribution of labeled bone marrow SPCs to hematopoiesis, we assessed GFP-labeling of differentiated bone marrow lineages over a four-week chase period. Again, no GFP-labeling of bone marrow cells was observed in vehicle-injected mice (Figure S2A). Ter119$^{+}$ erythroid cells, which actively express *Abcg2* (29), were extensively labeled at both week 9 and week 13 (Figure 1I, Figures S2B, and S2C). Labeling of all other bone marrow lineages that do not express *Abcg2* (31) increased significantly over the four-week chase period highlighting the contribution of endogenous bone marrow SPCs to hematopoiesis (Figure 1I, Figures S2B, and S2C).

Similar to isolated bone marrow SPCs, intestinal SPCs enrich for stem cells that give rise to all four intestinal lineages in cell culture(40, 43). To determine whether *Abcg2*-expressing SPCs enrich for endogenous stem cells required for intestinal homeostasis, we evaluated GFP-labeling in the ileum of Abgc2$^{MCM/+}$ R26$^{GFP/+}$ mice after a single injection of tamoxifen (Figure 1C). Three days after a single tamoxifen injection, there was extensive labeling of enterocytes throughout the villi with minimal labeling in the crypts (Figure 1J). In contrast to this pattern of labeling, four weeks after a single injection of tamoxifen, there was widespread labeling of intestinal cells in a striated pattern that extended from the base of crypts to the tips of villi (Figure 1K). Given the high turnover rate of intestinal epithelium and the archetypal pattern of GFP-labeling observed in the ileum(44), it was clear that long-term intestinal stem cells were labeled and lineage-traced *in vivo*. Taken together, these studies show that *Abcg2*-expressing SPCs enrich for endogenous stem cells that are integral for adult bone marrow and intestinal homeostasis.

## CSPCs are efficiently labeled.

After establishing the ability of the side population phenotype to identify endogenous stem cells in organs with continuous cellular turnover, we evaluated the role of SPCs in the heart, one of the least regenerative organs in the body. In Abgc2$^{MCM/+}$ R26$^{GFP/+}$ mice, cSPCs accounted for 1.5% of non-cardiomyocytes (Figures 2A and 2B), which was consistent with previous studies from other independent research groups(18, 22, 29). Moreover, cSPCs were efficiently labeled with 73.2 ± 9.8 % expressing GFP (Figure 2C, n=7).

To evaluate whether labeled cSPCs give rise to cardiac cells, we measured GFP-labeling of non-cardiomyocytes over a four-week chase period using flow cytometry and immunohistochemical staining. There was extensive labeling of cardiac endothelial cells, which are known to express *Abcg2*(41), with a small, but significant, increase in labeling over the four-week chase period (Figures 2D and 2E). Other non-cardiomyocyte lineages were less frequently labeled with no significant changes in labeling over time (Figure 2F-2L). Twenty percent of CD90$^{+}$ cells expressed GFP (Figure 2G); however, most of these cells were lymphatic endothelial cells that co-expressed CD31 and CD90 (PMID: 20599951 and 26987915) with only 4.0 ± 1.0% of fibroblasts (CD90$^{+}$ CD31$^{-}$ cells, n=4) labeled with GFP after a four-week chase period. Additionally, only 5.0 ± 3.1% of residential cardiac CD45$^{+}$ cells expressed GFP (Figures 2H and 2I, n=4) despite extensive bone marrow labeling (Figure 1I), which may reflect differences in labeling of embryonic and adult-derived macrophages residing in the heart(45).

## CSPCs contribute to cardiomyocyte labeling during cardiac homeostasis.

While assessing labeling in the heart, we observed GFP-labeled cardiomyocytes in histological sections and adult cardiomyocyte isolations (Figures 3A and 3B). To quantify the contribution of cSPCs to lineage-traced cardiomyocytes, we measured GFP-labeling of isolated adult cardiomyocytes over a four-week chase period. Over this time period, we found a five-fold increase in cardiomyocyte labeling from 0.18% to 0.84% (Figures 3C-3F). Although we did not observe active mRNA or protein expression of Abcg2 in adult cardiomyocytes with qPCR and immunohistochemistry (Figure 1D and Figure S3), we performed a more rigorous experiment to assess whether cardiomyocyte labeling arose from

lineage-tracing of *Abcg2*-expressing cSPCs or from *Abcg2*-expression by cardiomyocytes. We did this by evaluating GFP-labeling of cardiomyocytes 72 hours and four weeks after a single tamoxifen injection (Figure 3G). Cardiomyocytes that actively expressed *Abcg2* would express GFP at the 72-hour time point while cardiomyocytes derived from *Abcg2*-expressing cSPCs would be labeled with GFP at the four-week time point. At 72 hours, only 0.03% of cardiomyocytes expressed GFP, which increased to 0.74% four weeks later (Figure 3H). These results provided further evidence that lineage-traced cardiomyocytes arose from cSPCs and not active *Abcg2* expression in cardiomyocytes.

To assess the function of lineage-traced cardiomyocytes, we measured cytoplasmic calcium ($cCa^{2+}$) dynamics and contractility in isolated adult cardiomyocytes under baseline conditions and in response to isoproterenol stimulation. We observed normal $Ca^{2+}$ cycling, fractional shortening, and adrenergic responsiveness of labeled cardiomyocytes with no difference in $cCa^{2+}$ dynamics and contractility between labeled and unlabeled cardiomyocytes (Figures 3I-3O). These data demonstrate that *Abcg2*-expressing cells contribute to labeling of fully-functional adult cardiomyocytes in the uninjured heart.

## Bone marrow cells and endothelial cells do not give rise to cardiomyocyte labeling.

Since bone-marrow-derived cells were extensively labeled in $Abcg2^{MCM/+}$ $R26^{GFP/+}$ mice and have been reported to give rise to cardiomyocytes(46, 47), we next evaluated the contribution of lineage-traced bone marrow SPCs to labeled cardiomyocytes. We generated bone marrow chimeras by transplanting irradiated Myh7-Cre $R26^{tdTomato/+}$ mice with bone marrow HSCs isolated from $Abcg2^{MCM/+}$ $R26^{GFP/+}$ mice (Figure 4A). We waited ten weeks after transplantation to allow sufficient time for transplanted HSCs to engraft and reconstitute the bone marrow niche before injecting chimeric mice with tamoxifen (Figure 4B). After a four-week chase period, labeling of bone marrow cells in chimeric mice was comparable to bone marrow labeling in $Abcg2^{MCM/+}$ $R26^{GFP/+}$ mice at week 13 (Figures 1H, Figure 1I and Table 1), confirming successful engraftment and lineage-tracing of bone marrow SPCs. In the hearts of chimeric mice, we rarely observed GFP-labeled cardiomyocytes (Figure 4C, 0.02 ± 0.03%, n=5). All GFP-labeled cardiomyocytes also expressed tdTomato, indicating that they arose from fusion of GFP-labeled bone-marrow-derived cells with preexisting tdTomato-labeled cardiomyocytes (Figure 4C). These transplantation studies show that bone marrow cells are not the source of cardiomyocyte labeling in $Abcg2^{MCM/+}$ $R26^{GFP/+}$ mice.

Cardiac endothelial cells have also been shown to contribute to cardiomyocytes in the adult heart(48, 49). To assess whether GFP-labeled endothelial cells contribute to cardiomyocyte-labeling, we evaluated cardiomyocyte labeling in BAC-Cdh5-CreERT2 mice, an endothelial-specific(32) transgenic tamoxifen-inducible Cre mouse model (Figures 4D and 4E). Four weeks after tamoxifen treatment, endothelial cells were efficiently labeled with GFP in BAC-Cdh5-CreERT2 $R26^{GFP/+}$ mice (Figure 4F); however, no GFP-labeled cardiomyocytes were identified, indicating that endothelial cells do not account for the observed cardiomyocyte labeling in $Abcg2^{MCM/+}$ $R26^{GFP/+}$ mice (Figure 4G). Taken together, these studies demonstrate that *Abcg2*-expressing cSPCs, not bone marrow or endothelial cells, contribute to lineage-traced cardiomyocytes under homeostatic conditions.

### Cardiac injury increases cSPC contribution to cardiomyocyte labeling.

Next, we assessed how different forms of cardiac injury influence the contribution of cSPCs to lineage-traced cardiomyocytes. Since cSPCs and endogenous cardiac regeneration are both activated in response to myocardial ischemic (MI) injury (13, 20, 22, 50), we permanently ligated the left coronary artery in Abcg2$^{MCM/+}$ R26$^{GFP/+}$ mice and analyzed GFP-labeling of cardiomyocytes from histological sections four weeks later (Figure 5A-5B). Cardiomyocyte labeling was significantly higher four weeks after MI compared to four weeks after sham operation (Figures 5C-5E). To ensure that the cardiomyocyte labeling we observed did not arise from cardiomyocytes expressing ABCG2 following MI injury, we stained sections from wild type mice 72 hours after MI injury (Figure S4A). We did not detect any cardiomyocytes that expressed ABCG2 within the border zones or remote regions of MI-injured hearts (Figures S4B-S4C). Additionally, we found that cardiac endothelial cells were extensively labeled throughout MI-injured hearts with minimal labeling of fibroblasts and hematopoietic cells (Figures 5F, 5G and S4D).

We also assessed how acute isoproterenol-induced cardiac injury(51, 52) impacted lineage-tracing of cardiomyocytes (Figures S5A). Similar to the response following MI, there was a higher percentage of cardiomyocytes labeled in isoproterenol-injected mice compared to saline-injected controls (Figure S5B and S5C). These data demonstrate that the contribution of cSPCs to cardiomyocytes is further enhanced in response to different forms of cardiac injury.

### CSPCs fuse with preexisting cardiomyocytes to stimulate cardiomyocyte cell cycle reentry.

Finally, we assessed the cellular mechanisms by which *Abcg2*-expressing cSPCs contributed to cardiomyocyte labeling. To more stringently determine whether lineage-traced cardiomyocytes were newly formed, we injected EdU with tamoxifen into Abcg2$^{MCM/+}$ R26$^{GFP/+}$ mice and assessed EdU incorporation four weeks later (Figure S6A). We observed EdU incorporation in nuclei of GFP-labeled cardiomyocytes and non-cardiomyocytes on histological sections (Figures S6B). To accurately identify and quantify EdU-incorporation and nucleation of GFP-labeled cardiomyocytes, we again injected EdU and tamoxifen into Abcg2$^{MCM/+}$ R26$^{GFP/+}$ mice and quantified EdU incorporation, GFP-labeling and nucleation in isolated adult cardiomyocytes (Figures 6A). There was no difference in the nucleation of GFP$^{+}$ and GFP$^{-}$ cardiomyocytes (Figures S7). We observed EdU incorporation in 0.0012% of all isolated adult cardiomyocytes, which translated to an overall cardiomyocyte DNA synthesis rate of 0.77% per year (Figure S8), consistent with previous studies(13). Importantly, EdU$^{+}$ cardiomyocytes were enriched for lineage-traced cardiomyocytes with 21% expressing GFP compared to only 0.7% of all cardiomyocytes expressing GFP. There was enrichment for lineage-traced cardiomyocytes in both mononucleated and binucleated EdU$^{+}$ cardiomyocytes (Figure 6B-6D). These data clearly show that *Abcg2*-expressing SPCs contribute to cardiomyocyte cell cycle reentry and, possibly, new cardiomyocyte formation.

In addition to directly differentiating into cardiomyocytes, transplanted cardiac progenitor cells have been shown to fuse with preexisting cardiomyocytes(53). To assess whether lineage-traced cardiomyocytes arise from direct differentiation of cSPCs and/or fusion with

cSPCs, we cross-bred Abcg2$^{MCM/+}$ mice with R26$^{mTom\text{-}mGFP/\ mTom\text{-}mGFP}$ reporter mice (Figure 6E). In Abcg2$^{MCM/+}$ R26$^{mTom\text{-}mGFP/+}$ mice, membrane-bound tdTomato (mTom) is expressed in all cells prior to recombination and membrane-bound GFP (mGFP) is expressed following recombination. Seventy-two hours after tamoxifen injections, all mGFP labeled cardiomyocytes also expressed mTom. After a four-week chase period, 85.3% of GFP-labeled cardiomyocytes were mTom$^+$ indicating that they likely arose from fusion events, while 14.6% did not express mTom indicating that they potentially arose from direct differentiation of cSPCs to cardiomyocytes (Figures 6F and 6G). Importantly, we did not detect differences in cross-sectional area of mGFP$^+$mTom$^-$, mGFP$^+$mTom$^+$, or mGFP$^-$mTom$^+$ cardiomyocytes (data not shown).

In cell culture, there is evidence that fusion between cardiomyocytes and non-cardiomyocytes can trigger cardiomyocyte cell-cycle reentry(49). Since lineage-traced cardiomyocytes arise from fusion with *Abcg2*-expressing non-cardiomyocytes (Figure 6B and C), we wanted to assess if fusion triggered cardiomyocytes to reenter the cell cycle in our mouse model. We first repeated our EdU incorporation studies in Abcg2$^{MCM/+}$ R26$^{mTom\text{-}mGFP/+}$ mice, which we had previously used to study cardiomyocyte fusion; however, we were unable to accurately identify mTom$^+$ and mGFP$^+$ cardiomyocytes because of the high background autofluorescence in fixed, isolated adult cardiomyocytes required for EdU incorporation studies. Therefore, we generated another mouse line, Abcg2$^{MCM/+}$ R26$^{nTom\text{-}nGFP/+}$, to perform our EdU-incorporation experiments with (Figure 6H). In this mouse model nuclear-localized tdTomato (nTom) is expressed in all cells prior to recombination and nuclear-localized GFP (nGFP) is expressed following recombination. The nuclear-localized fluorophores allowed for accurate identification of nGFP$^+$ and nTom$^+$ cardiomyocytes in fixed samples. We first confirmed that the same level of fusion occurred in this model with 86% of nGFP$^+$ cardiomyocytes co-expressing nTom (Figure S9A). Next, we performed EdU incorporation studies and found a significant enrichment of nGFP labeling in EdU$^+$ cardiomyocytes, with 13% expressing nGFP (Figure S9B and S9C). Importantly, we found that all EdU$^+$ lineage-traced cardiomyocytes expressed both nTom and nGFP (Figure 6I). These findings show that all lineage-traced cardiomyocytes that reentered the cell cycle arose from fusion with *Abcg2*-expressing non-cardiomyocytes and not differentiation of an *Abcg2*-expressing progenitor cell population.

## DISCUSSION

Evidence supporting the existence of endogenous cardiac regeneration, the heart's innate ability to form new cells, opened up opportunities for regenerating the failing heart. Previously, the adult mammalian heart was believed to be a post-mitotic organ that could not generate new cardiomyocytes; however, in the past ten years, studies in mice and humans have convincingly demonstrated that a small number of new cardiomyocytes are formed after birth(13, 50, 54, 55). Unfortunately, the number of cardiomyocytes generated is not sufficient to compensate for those lost during the progression of heart failure. Future therapies that enhance endogenous cardiac regeneration have the potential to improve clinical outcomes.

There are two main groups of cells that have been studied to enhance endogenous cardiac regeneration – cardiac progenitor cells and proliferating cardiomyocytes. Cardiac progenitor cells were thought to have the advantage of giving rise to non-cardiomyocytes and cardiomyocytes, both of which are integral to normal cardiac function(56, 57); however, recent evidence suggests that these cells may be incapable of generating cardiomyocytes(4, 14, 58) and there is now a concerted effort to enhancing endogenous cardiac regeneration by stimulating cardiomyocyte proliferation(59, 60). Moreover, growing evidence has accumulated that *Kit*-expressing cells, the most extensively studied group of proposed cardiac progenitor cells, have a negligible contribution to endogenous cardiac regeneration(10, 11, 15). For these reasons, we set out to evaluate the role of other proposed progenitor cells that are distinct from cardiac *Kit*-expressing cells. We chose to study the regenerative potential of endogenous cSPCs because they do not express *Kit* at the mRNA or protein level(24, 61). Furthermore, high-throughput transcriptional analysis comparing cardiac *Kit*-expressing cells to cSPCs demonstrated a striking difference in expression profiles between these two populations of cells(27).

Here, we used a genetic lineage-tracing approach to investigate whether cSPCs enrich for endogenous residential non-cardiomyocytes that give rise to cardiomyocytes during cardiac homeostasis and in response to cardiac injury. We used *Abcg2*-expression to lineage-trace SPCs since studies have shown that ABCG2 is essential for the side population phenotype but not required for the stem cell function of SPCs under homeostatic conditions(19, 30, 31). In bone marrow SPCs, ABCG2 is the only ABC transporter responsible for the side population phenotype(30). In the adult heart, ABCG2 and p-glycoprotein, which is encoded by *Mdr1a* and *Mdr1b*, are both responsible for the side population phenotype(29). When *Abcg2* is knocked out, mice are viable with no defects in bone marrow or cardiac homeostasis(29, 30). For this reason, we used an *Abcg2*-driven lineage-tracing mouse model to trace SPCs *in vivo* to determine whether they are enriched for endogenous stem cells in the heart and other tissues throughout the body.

With our *Abcg2*-driven, lineage-tracing approach, we showed that SPCs enrich for endogenous stem cells that are critical for bone marrow and intestinal homeostasis. The level of labeling we observed was much higher than a previous attempt to lineage-trace bone marrow SPCs, where only 2–3% of bone marrow SPCs, LSK cells and differentiated lineages were labeled up to a year after tamoxifen induction(62). This previous model inefficiently labeled *Abcg2*-expressing cells most likely because it used an IRES-dependent approach to drive translation of both ABCG2 and CreERT2 from the same mRNA. Our knock-in genetic strategy efficiently labeled *Abcg2*-expressing cells because we replaced the ATG containing exon of the *Abcg2* gene with MerCreMer cDNA.

With our mouse model, we showed that *Abcg2*-expressing cSPCs contribute to lineage-traced cardiomyocytes during cardiac homeostasis with increased contribution following isoproterenol-induced and MI injury. We demonstrated that lineage-traced bone marrow cells and endothelial cells do not contribute to cardiomyocyte labeling. More importantly, we found that cardiac SPCs fuse with preexisting cardiomyocytes and induce cell cycle reentry in lineage-traced cardiomyocytes. Our findings build on previous reports of cardiomyocyte fusion with non-cardiomyocytes(61, 63-66). In cell culture, cardiomyocytes

have the potential to fuse with endothelial cells and fibroblasts(49). These findings were corroborated by genetic lineage tracing of cardiomyocytes, which showed that almost 2% of cardiomyocytes in the adult heart arise from fusion with unidentified non-cardiomyocytes(50). Subsequent studies identified multiple cell types, including circulating bone marrow cells, Sca-$1^+$ cells, and c-$kit^+$ cells, that have the potential to fuse with cardiomyocytes(11, 15, 53, 63, 65, 66). Our results extend these findings by providing evidence that residential *Abcg2*-expressing non-cardiomyocytes fuse with pre-existing cardiomyocytes at rates that account for most cardiomyocyte fusion events reported by Hsieh et al.(50).

While fusion and proliferation have been thought of as distinct processes, there is growing evidence that cardiomyocyte fusion can trigger cell cycle entry and induce cardiomyocyte proliferation. Transient membrane fusion between cardiomyocytes has been shown to be essential for cardiomyocyte proliferation in adult zebrafish(67). When cardiomyocytes are co-cultured with endothelial cells and fibroblasts, they fuse with surrounding non-cardiomyocytes, re-enter the cell cycle, and begin to proliferate(49). In a recent study, *Twist2*-expressing non-cardiomyocytes were shown to fuse with preexisting cardiomyocytes; however, the relationship between fusion and cardiomyocyte proliferation was not assessed in this study(68). In our study, we used the side population phenotype to identify a population of residential non-cardiomyocytes that fuse with preexisting cardiomyocytes to trigger cardiomyocyte cell cycle reentry. When we consider our findings within the context of recently published studies, we believe that fusion between cardiomyocytes and non-cardiomyocytes regulates endogenous cardiomyocyte proliferation in the adult mammalian heart.

The main limitation of our study is that we cannot conclusively rule out *Abcg2*-expression in a small number of cardiomyocytes. In two previously published studies, researchers found ABCG2 expressed at the protein level in diseased human hearts; however, these studies did not determine whether ABCG2 was expressed by cardiomyocytes or non-cardiomyocytes (69-71). Additionally, the appropriate negative controls were not available for these human samples to verify specificity of the methodologies used (69-71). In our studies, we did not observe expression of Abcg2 at the mRNA or protein level with qPCR or immunohistochemistry, respectively. We used cardiac tissue from *Abcg2* knockout mice to rigorously evaluate the specificity of four commercially available ABCG2 antibodies and found that only one antibody specifically bound ABCG2. We also used internal controls to confirm the purity of our cardiomyocyte and endothelial samples used for qPCR analysis. Furthermore, our study with single tamoxifen injections provided additional evidence that the increase in GFP-labeling of cardiomyocytes over the four-week chase period arises from the contribution of *Abcg2*-expressing cells to cardiomyocytes and not from active expression of *Abcg2* by cardiomyocytes. Despite the care we took with our studies, it is impossible to prove that cardiomyocytes never express *Abcg2*. If a small percentage of cardiomyocytes do express *Abcg2*, our data would suggest that these cardiomyocytes represent a more proliferative population of cardiomyocytes since GFP-labeled cardiomyocytes have higher rates of EdU incorporation.

Another limitation of our study is that other *Abcg2*-expressing non-cardiomyocytes are lineage-traced in our mouse model. Currently, there is no unique marker for SPCs and future studies will be needed to identify a specific SPC marker. Because endothelial and bone-marrow derived cells are labeled with GFP, we generated two mouse lines to allow us to critically evaluate the contribution of these cells types to lineage-traced cardiomyocytes. With our endothelial cell lineage-tracing mouse model, we showed that labeled endothelial cells do not give rise to any lineage-traced cardiomyocytes. In our bone marrow chimera studies, we did observe rare fusion events between preexisting cardiomyocytes and labeled bone-marrow-derived cells as previously reported by other groups (61, 63-66), but not enough to account for most of the lineage-traced cardiomyocytes we identified. With these approaches, we showed that *Abcg2*-expressing endothelial and bone-marrow derived cells do not contribute to lineage-traced cardiomyocytes.

Our study is the first to show that residential *Abcg2*-expressing non-cardiomyocytes identified by the side population phenotype fuse with cardiomyocytes to trigger cell-cycle reentry *in vivo*. This mechanism may account for as much as 20% of newly-generated cardiomyocytes in the adult heart. Further research is needed to characterize *Abcg2*-expressing fusogenic non-cardiomyocytes and to understand their relationship with other cells in the heart(68). Moving forward, we will need to carefully study how fusion triggers cell-cycle reentry in cardiomyocytes and whether this mechanism can be targeted for future regenerative therapies.

## Supplementary Material

Refer to Web version on PubMed Central for supplementary material.

## ACKNOWLEDGMENTS

The authors would like to thank Xiaodan Wang, Natsumi Nemoto, Chetana Guthikonda, Jessica Shaklee, Wuqiang Zhu, Ingrid Bender, and John Calvert for their assistance. This work was supported by the National Institutes of Health (HL112852, HL130072 to J.H.van Berlo and MSTP T32GM008244 to A.Yellamilli). J.H.van Berlo is supported by The Hartwell Foundation and Minnesota Regenerative Medicine Initiative.

## NONSTANDARD ABBREVIATIONS

| | |
|---|---|
| **ABC** | ATP-Binding Cassette (superfamily of transporter proteins) |
| **ABCG2** | ATP-Binding Cassette Subfamily G Member 2 protein |
| **Abcg2** | ATP-Binding Cassette Subfamily G Member 2 gene |
| **BAC** | Bacterial Artificial Chromosome |
| **bmSPC** | bone marrow Side Population Cell |
| **CM** | Cardiomyocyte |
| **cSPC** | cardiac Side Population Cell |
| **EdU** | 5-Ethynyl-2’-deoxyUridine (thymidine analog) |

| | |
|---|---|
| **EC** | Endothelial cell |
| **FACS** | Flow Assisted Cell Sorting |
| **GFP** | Green Fluorescent Protein |
| **HSC** | Hematopoietic Stem Cell |
| **ISO** | Isoproterenol |
| **LSK** | Lineage marker$^{-}$, Sca-1$^{+}$, Kit$^{+}$ Cells |
| **MCM** | MerCreMer (a Cre recombinase protein flanked by mutated estrogen receptors) |
| **mGFP** | membrane-targeted GFP protein |
| **MI** | Myocardial ischemia |
| **mTom** | membrane-targeted Tomato protein |
| **nGFP** | nuclear-targeted GFP protein |
| **nTom** | nuclear-targeted Tomato protein |
| **SD** | Standard Deviation |
| **SP** | Side Population |
| **SPC** | Side Population Cell |
| **Tom** | Tomato protein |
| **Wk** | Week |

## REFERENCES


1. Chiong M, Wang ZV, Pedrozo Z, Cao DJ, Troncoso R, Ibacache M, Criollo A, Nemchenko A, Hill JA, and Lavandero S (2011) Cardiomyocyte death: mechanisms and translational implications. Cell Death Dis 2, e244 [PubMed: 22190003]
2. van Empel VP, Bertrand AT, Hofstra L, Crijns HJ, Doevendans PA, and De Windt LJ (2005) Myocyte apoptosis in heart failure. Cardiovasc Res 67, 21–29 [PubMed: 15896727]
3. Tzahor E, and Poss KD (2017) Cardiac regeneration strategies: Staying young at heart. Science 356, 1035–1039 [PubMed: 28596337]
4. van Berlo JH, and Molkentin JD (2014) An emerging consensus on cardiac regeneration. Nat Med 20, 1386–1393 [PubMed: 25473919]
5. Epstein JA (2019) A Time to Press Reset and Regenerate Cardiac Stem Cell Biology. JAMA Cardiol 4, 95–96 [PubMed: 30480702]
6. Beltrami AP, Barlucchi L, Torella D, Baker M, Limana F, Chimenti S, Kasahara H, Rota M, Musso E, Urbanek K, Leri A, Kajstura J, Nadal-Ginard B, and Anversa P (2003) Adult cardiac stem cells are multipotent and support myocardial regeneration. Cell 114, 763–776 [PubMed: 14505575]
7. Hong KU, Guo Y, Li QH, Cao P, Al-Maqtari T, Vajravelu BN, Du J, Book MJ, Zhu X, Nong Y, Bhatnagar A, and Bolli R (2014) c-kit+ Cardiac stem cells alleviate post-myocardial infarction left ventricular dysfunction despite poor engraftment and negligible retention in the recipient heart. PLoS One 9, e96725 [PubMed: 24806457]

8. Liu Q, Yang R, Huang X, Zhang H, He L, Zhang L, Tian X, Nie Y, Hu S, Yan Y, Qiao Z, Wang QD, Lui KO, and Zhou B (2016) Genetic lineage tracing identifies in situ Kit-expressing cardiomyocytes. Cell Res 26, 119–130 [PubMed: 26634606]

9. Sanganalmath SK, and Bolli R (2013) Cell therapy for heart failure: a comprehensive overview of experimental and clinical studies, current challenges, and future directions. Circ Res 113, 810–834 [PubMed: 23989721]

10. Sultana N, Zhang L, Yan J, Chen J, Cai W, Razzaque S, Jeong D, Sheng W, Bu L, Xu M, Huang GY, Hajjar RJ, Zhou B, Moon A, and Cai CL (2015) Resident c-kit(+) cells in the heart are not cardiac stem cells. Nat Commun 6, 8701 [PubMed: 26515110]

11. van Berlo JH, Kanisicak O, Maillet M, Vagnozzi RJ, Karch J, Lin SC, Middleton RC, Marbán E, and Molkentin JD (2014) c-kit+ cells minimally contribute cardiomyocytes to the heart. Nature 509, 337–341 [PubMed: 24805242]

12. Eschenhagen T, Bolli R, Braun T, Field LJ, Fleischmann BK, Frisén J, Giacca M, Hare JM, Houser S, Lee RT, Marbán E, Martin JF, Molkentin JD, Murry CE, Riley PR, Ruiz-Lozano P, Sadek HA, Sussman MA, and Hill JA (2017) Cardiomyocyte Regeneration: A Consensus Statement. Circulation 136, 680–686 [PubMed: 28684531]

13. Senyo SE, Steinhauser ML, Pizzimenti CL, Yang VK, Cai L, Wang M, Wu TD, Guerquin-Kern JL, Lechene CP, and Lee RT (2013) Mammalian heart renewal by pre-existing cardiomyocytes. Nature 493, 433–436 [PubMed: 23222518]

14. Li Y, He L, Huang X, Bhaloo SI, Zhao H, Zhang S, Pu W, Tian X, Liu Q, Yu W, Zhang L, Liu X, Liu K, Tang J, Zhang H, Cai D, Ralf AH, Xu Q, Lui KO, and Zhou B (2018) Genetic Lineage Tracing of Nonmyocyte Population by Dual Recombinases. Circulation 138, 793–805 [PubMed: 29700121]

15. He L, Li Y, Pu W, Huang X, Tian X, Wang Y, Zhang H, Liu Q, Zhang L, Zhao H, Tang J, Ji H, Cai D, Han Z, Nie Y, Hu S, Wang QD, Sun R, Fei J, Wang F, Chen T, Yan Y, Huang H, Pu WT, and Zhou B (2017) Enhancing the precision of genetic lineage tracing using dual recombinases. Nat Med 23, 1488–1498 [PubMed: 29131159]

16. Kretzschmar K, Post Y, Bannier-Hélaouët M, Mattiotti A, Drost J, Basak O, Li VSW, van den Born M, Gunst QD, Versteeg D, Kooijman L, van der Elst S, van Es JH, van Rooij E, van den Hoff MJB, and Clevers H (2018) Profiling proliferative cells and their progeny in damaged murine hearts. Proc Natl Acad Sci U S A 115, E12245–E12254 [PubMed: 30530645]

17. Golebiewska A, Brons NH, Bjerkvig R, and Niclou SP (2011) Critical appraisal of the side population assay in stem cell and cancer stem cell research. Cell Stem Cell 8, 136–147 [PubMed: 21295271]

18. Hierlihy AM, Seale P, Lobe CG, Rudnicki MA, and Megeney LA (2002) The post-natal heart contains a myocardial stem cell population. FEBS Lett 530, 239–243 [PubMed: 12387899]

19. Martin CM, Meeson AP, Robertson SM, Hawke TJ, Richardson JA, Bates S, Goetsch SC, Gallardo TD, and Garry DJ (2004) Persistent expression of the ATP-binding cassette transporter, Abcg2, identifies cardiac SP cells in the developing and adult heart. Dev Biol 265, 262–275 [PubMed: 14697368]

20. Unno K, Jain M, and Liao R (2012) Cardiac side population cells: moving toward the center stage in cardiac regeneration. Circ Res 110, 1355–1363 [PubMed: 22581921]

21. Goodell MA, Brose K, Paradis G, Conner AS, and Mulligan RC (1996) Isolation and functional properties of murine hematopoietic stem cells that are replicating in vivo. J Exp Med 183, 1797–1806 [PubMed: 8666936]

22. Yellamilli A, and van Berlo JH (2016) The Role of Cardiac Side Population Cells in Cardiac Regeneration. Front Cell Dev Biol 4, 102 [PubMed: 27679798]

23. Oyama T, Nagai T, Wada H, Naito AT, Matsuura K, Iwanaga K, Takahashi T, Goto M, Mikami Y, Yasuda N, Akazawa H, Uezumi A, Takeda S, and Komuro I (2007) Cardiac side population cells have a potential to migrate and differentiate into cardiomyocytes in vitro and in vivo. J Cell Biol 176, 329–341 [PubMed: 17261849]

24. Noseda M, Harada M, McSweeney S, Leja T, Belian E, Stuckey DJ, Abreu Paiva MS, Habib J, Macaulay I, de Smith AJ, al-Beidh F, Sampson R, Lumbers RT, Rao P, Harding SE, Blakemore AI, Jacobsen SE, Barahona M, and Schneider MD (2015) PDGFRα demarcates the cardiogenic

clonogenic Sca1+ stem/progenitor cell in adult murine myocardium. Nat Commun 6, 6930 [PubMed: 25980517]

25. Pfister O, Mouquet F, Jain M, Summer R, Helmes M, Fine A, Colucci WS, and Liao R (2005) CD31- but Not CD31+ cardiac side population cells exhibit functional cardiomyogenic differentiation. Circ Res 97, 52–61 [PubMed: 15947249]
26. Liang SX, Tan TY, Gaudry L, and Chong B (2010) Differentiation and migration of Sca1+/CD31- cardiac side population cells in a murine myocardial ischemic model. Int J Cardiol 138, 40–49 [PubMed: 19254813]
27. Dey D, Han L, Bauer M, Sanada F, Oikonomopoulos A, Hosoda T, Unno K, De Almeida P, Leri A, and Wu JC (2013) Dissecting the molecular relationship among various cardiogenic progenitor cells. Circ Res 112, 1253–1262 [PubMed: 23463815]
28. Krishnamurthy P, and Schuetz JD (2006) Role of ABCG2/BCRP in biology and medicine. Annu Rev Pharmacol Toxicol 46, 381–410 [PubMed: 16402910]
29. Pfister O, Oikonomopoulos A, Sereti KI, Sohn RL, Cullen D, Fine GC, Mouquet F, Westerman K, and Liao R (2008) Role of the ATP-binding cassette transporter Abcg2 in the phenotype and function of cardiac side population cells. Circ Res 103, 825–835 [PubMed: 18787193]
30. Zhou S, Morris JJ, Barnes Y, Lan L, Schuetz JD, and Sorrentino BP (2002) Bcrp1 gene expression is required for normal numbers of side population stem cells in mice, and confers relative protection to mitoxantrone in hematopoietic cells in vivo. Proc Natl Acad Sci U S A 99, 12339–12344 [PubMed: 12218177]
31. Zhou S, Schuetz JD, Bunting KD, Colapietro AM, Sampath J, Morris JJ, Lagutina I, Grosveld GC, Osawa M, Nakauchi H, and Sorrentino BP (2001) The ABC transporter Bcrp1/ABCG2 is expressed in a wide variety of stem cells and is a molecular determinant of the side-population phenotype. Nat Med 7, 1028–1034 [PubMed: 11533706]
32. Okabe K, Kobayashi S, Yamada T, Kurihara T, Tai-Nagara I, Miyamoto T, Mukouyama YS, Sato TN, Suda T, Ema M, and Kubota Y (2014) Neurons limit angiogenesis by titrating VEGF in retina. Cell 159, 584–596 [PubMed: 25417109]
33. Parsons SA, Millay DP, Wilkins BJ, Bueno OF, Tsika GL, Neilson JR, Liberatore CM, Yutzey KE, Crabtree GR, Tsika RW, and Molkentin JD (2004) Genetic loss of calcineurin blocks mechanical overload-induced skeletal muscle fiber type switching but not hypertrophy. J Biol Chem 279, 26192–26200 [PubMed: 15082723]
34. Gundewar S, Calvert JW, Elrod JW, and Lefer DJ (2007) Cytoprotective effects of N,N,N-trimethylsphingosine during ischemia- reperfusion injury are lost in the setting of obesity and diabetes. Am J Physiol Heart Circ Physiol 293, H2462–2471 [PubMed: 17630348]
35. Ergen AV, Jeong M, Lin KK, Challen GA, and Goodell MA (2013) Isolation and characterization of mouse side population cells. Methods Mol Biol 946, 151–162 [PubMed: 23179831]
36. Pfister O, Oikonomopoulos A, Sereti KI, and Liao R (2010) Isolation of resident cardiac progenitor cells by Hoechst 33342 staining. Methods Mol Biol 660, 53–63 [PubMed: 20680812]
37. O'Connell TD, Rodrigo MC, and Simpson PC (2007) Isolation and culture of adult mouse cardiac myocytes. Methods Mol Biol 357, 271–296 [PubMed: 17172694]
38. Chen Z, Zhu W, Bender I, Gong W, Kwak IY, Yellamilli A, Hodges TJ, Nemoto N, Zhang J, Garry DJ, and van Berlo JH (2017) Pathologic Stimulus Determines Lineage Commitment of Cardiac C-kit. Circulation 136, 2359–2372 [PubMed: 29021323]
39. Luongo TS, Lambert JP, Gross P, Nwokedi M, Lombardi AA, Shanmughapriya S, Carpenter AC, Kolmetzky D, Gao E, van Berlo JH, Tsai EJ, Molkentin JD, Chen X, Madesh M, Houser SR, and Elrod JW (2017) The mitochondrial Na+/Ca2+ exchanger is essential for Ca2+ homeostasis and viability. Nature 545, 93–97 [PubMed: 28445457]
40. Dekaney CM, Rodriguez JM, Graul MC, and Henning SJ (2005) Isolation and characterization of a putative intestinal stem cell fraction from mouse jejunum. Gastroenterology 129, 1567–1580 [PubMed: 16285956]
41. Higashikuni Y, Sainz J, Nakamura K, Takaoka M, Enomoto S, Iwata H, Sahara M, Tanaka K, Koibuchi N, Ito S, Kusuhara H, Sugiyama Y, Hirata Y, Nagai R, and Sata M (2010) The ATP-binding cassette transporter BCRP1/ABCG2 plays a pivotal role in cardiac repair after myocardial

infarction via modulation of microvascular endothelial cell survival and function. Arterioscler Thromb Vasc Biol 30, 2128–2135 [PubMed: 20829509]

42. Horsey AJ, Cox MH, Sarwat S, and Kerr ID (2016) The multidrug transporter ABCG2: still more questions than answers. Biochem Soc Trans 44, 824–830 [PubMed: 27284047]
43. von Furstenberg RJ, Buczacki SJ, Smith BJ, Seiler KM, Winton DJ, and Henning SJ (2014) Side population sorting separates subfractions of cycling and non-cycling intestinal stem cells. Stem Cell Res 12, 364–375 [PubMed: 24365601]
44. Darwich AS, Aslam U, Ashcroft DM, and Rostami-Hodjegan A (2014) Meta-analysis of the turnover of intestinal epithelia in preclinical animal species and humans. Drug Metab Dispos 42, 2016–2022 [PubMed: 25233858]
45. Epelman S, Lavine KJ, Beaudin AE, Sojka DK, Carrero JA, Calderon B, Brija T, Gautier EL, Ivanov S, Satpathy AT, Schilling JD, Schwendener R, Sergin I, Razani B, Forsberg EC, Yokoyama WM, Unanue ER, Colonna M, Randolph GJ, and Mann DL (2014) Embryonic and adult-derived resident cardiac macrophages are maintained through distinct mechanisms at steady state and during inflammation. Immunity 40, 91–104 [PubMed: 24439267]
46. Deb A, Wang S, Skelding KA, Miller D, Simper D, and Caplice NM (2003) Bone marrow-derived cardiomyocytes are present in adult human heart: A study of gender-mismatched bone marrow transplantation patients. Circulation 107, 1247–1249 [PubMed: 12628942]
47. Jackson KA, Majka SM, Wang H, Pocius J, Hartley CJ, Majesky MW, Entman ML, Michael LH, Hirschi KK, and Goodell MA (2001) Regeneration of ischemic cardiac muscle and vascular endothelium by adult stem cells. J Clin Invest 107, 1395–1402 [PubMed: 11390421]
48. Fioret BA, Heimfeld JD, Paik DT, and Hatzopoulos AK (2014) Endothelial cells contribute to generation of adult ventricular myocytes during cardiac homeostasis. Cell Rep 8, 229–241 [PubMed: 25001281]
49. Matsuura K, Wada H, Nagai T, Iijima Y, Minamino T, Sano M, Akazawa H, Molkentin JD, Kasanuki H, and Komuro I (2004) Cardiomyocytes fuse with surrounding noncardiomyocytes and reenter the cell cycle. J Cell Biol 167, 351–363 [PubMed: 15492039]
50. Hsieh PC, Segers VF, Davis ME, MacGillivray C, Gannon J, Molkentin JD, Robbins J, and Lee RT (2007) Evidence from a genetic fate-mapping study that stem cells refresh adult mammalian cardiomyocytes after injury. Nat Med 13, 970–974 [PubMed: 17660827]
51. Brooks WW, and Conrad CH (2009) Isoproterenol-induced myocardial injury and diastolic dysfunction in mice: structural and functional correlates. Comp Med 59, 339–343 [PubMed: 19712573]
52. Wallner M, Duran JM, Mohsin S, Troupes CD, Vanhoutte D, Borghetti G, Vagnozzi RJ, Gross P, Yu D, Trappanese DM, Kubo H, Toib A, Sharp TE, Harper SC, Volkert MA, Starosta T, Feldsott EA, Berretta RM, Wang T, Barbe MF, Molkentin JD, and Houser SR (2016) Acute Catecholamine Exposure Causes Reversible Myocyte Injury Without Cardiac Regeneration. Circ Res 119, 865–879 [PubMed: 27461939]
53. Oh H, Bradfute SB, Gallardo TD, Nakamura T, Gaussin V, Mishina Y, Pocius J, Michael LH, Behringer RR, Garry DJ, Entman ML, and Schneider MD (2003) Cardiac progenitor cells from adult myocardium: homing, differentiation, and fusion after infarction. Proc Natl Acad Sci U S A 100, 12313–12318 [PubMed: 14530411]
54. Bergmann O, Bhardwaj RD, Bernard S, Zdunek S, Barnabe-Heider F, Walsh S, Zupicich J, Alkass K, Buchholz BA, Druid H, Jovinge S, and Frisen J (2009) Evidence for cardiomyocyte renewal in humans. Science 324, 98–102 [PubMed: 19342590]
55. Bergmann O, Zdunek S, Felker A, Salehpour M, Alkass K, Bernard S, Sjostrom SL, Szewczykowska M, Jackowska T, Dos Remedios C, Malm T, Andrä M, Jashari R, Nyengaard JR, Possnert G, Jovinge S, Druid H, and Frisén J (2015) Dynamics of Cell Generation and Turnover in the Human Heart. Cell 161, 1566–1575 [PubMed: 26073943]
56. Garbern JC, and Lee RT (2013) Cardiac stem cell therapy and the promise of heart regeneration. Cell Stem Cell 12, 689–698 [PubMed: 23746978]
57. Bollini S, Vieira JM, Howard S, Dubè KN, Balmer GM, Smart N, and Riley PR (2014) Re-activated adult epicardial progenitor cells are a heterogeneous population molecularly distinct from their embryonic counterparts. Stem Cells Dev 23, 1719–1730 [PubMed: 24702282]

58. van Berlo JH, and Molkentin JD (2016) Most of the Dust Has Settled: cKit+ Progenitor Cells Are an Irrelevant Source of Cardiac Myocytes In Vivo. Circ Res 118, 17–19 [PubMed: 26837741]
59. Leach JP, Heallen T, Zhang M, Rahmani M, Morikawa Y, Hill MC, Segura A, Willerson JT, and Martin JF (2017) Hippo pathway deficiency reverses systolic heart failure after infarction. Nature 550, 260–264 [PubMed: 28976966]
60. Nakada Y, Canseco DC, Thet S, Abdisalaam S, Asaithamby A, Santos CX, Shah AM, Zhang H, Faber JE, Kinter MT, Szweda LI, Xing C, Hu Z, Deberardinis RJ, Schiattarella G, Hill JA, Oz O, Lu Z, Zhang CC, Kimura W, and Sadek HA (2017) Hypoxia induces heart regeneration in adult mice. Nature 541, 222–227 [PubMed: 27798600]
61. Mouquet F, Pfister O, Jain M, Oikonomopoulos A, Ngoy S, Summer R, Fine A, and Liao R (2005) Restoration of cardiac progenitor cells after myocardial infarction by self-proliferation and selective homing of bone marrow-derived stem cells. Circ Res 97, 1090–1092 [PubMed: 16269652]
62. Fatima S, Zhou S, and Sorrentino BP (2012) Abcg2 expression marks tissue-specific stem cells in multiple organs in a mouse progeny tracking model. Stem Cells 30, 210–221 [PubMed: 22134889]
63. Nygren JM, Jovinge S, Breitbach M, Sawen P, Roll W, Hescheler J, Taneera J, Fleischmann BK, and Jacobsen SE (2004) Bone marrow-derived hematopoietic cells generate cardiomyocytes at a low frequency through cell fusion, but not transdifferentiation. Nat Med 10, 494–501 [PubMed: 15107841]
64. Murry CE, Soonpaa MH, Reinecke H, Nakajima H, Nakajima HO, Rubart M, Pasumarthi KB, Virag JI, Bartelmez SH, Poppa V, Bradford G, Dowell JD, Williams DA, and Field LJ (2004) Haematopoietic stem cells do not transdifferentiate into cardiac myocytes in myocardial infarcts. Nature 428, 664–668 [PubMed: 15034593]
65. Alvarez-Dolado M, Pardal R, Garcia-Verdugo JM, Fike JR, Lee HO, Pfeffer K, Lois C, Morrison SJ, and Alvarez-Buylla A (2003) Fusion of bone-marrow-derived cells with Purkinje neurons, cardiomyocytes and hepatocytes. Nature 425, 968–973 [PubMed: 14555960]
66. Wu JM, Hsueh YC, Ch'ang HJ, Luo CY, Wu LW, Nakauchi H, and Hsieh PC (2015) Circulating cells contribute to cardiomyocyte regeneration after injury. Circ Res 116, 633–641 [PubMed: 25398235]
67. Sawamiphak S, Kontarakis Z, Filosa A, Reischauer S, and Stainier DYR (2017) Transient cardiomyocyte fusion regulates cardiac development in zebrafish. Nat Commun 8, 1525 [PubMed: 29142194]
68. Min YL, Jaichander P, Sanchez-Ortiz E, Bezprozvannaya S, Malladi VS, Cui M, Wang Z, Bassel-Duby R, Olson EN, and Liu N (2018) Identification of a multipotent Twist2-expressing cell population in the adult heart. Proc Natl Acad Sci U S A 115, E8430–E8439 [PubMed: 30127033]
69. Alfakir M, Dawe N, Eyre R, Tyson-Capper A, Britton K, Robson SC, and Meeson AP (2012) The temporal and spatial expression patterns of ABCG2 in the developing human heart. Int J Cardiol 156, 133–138 [PubMed: 21111494]
70. Meissner K, Heydrich B, Jedlitschky G, Meyer Zu Schwabedissen H, Mosyagin I, Dazert P, Eckel L, Vogelgesang S, Warzok RW, Böhm M, Lehmann C, Wendt M, Cascorbi I, and Kroemer HK (2006) The ATP-binding cassette transporter ABCG2 (BCRP), a marker for side population stem cells, is expressed in human heart. J Histochem Cytochem 54, 215–221 [PubMed: 16116030]
71. Solbach TF, Paulus B, Weyand M, Eschenhagen T, Zolk O, and Fromm MF (2008) ATP-binding cassette transporters in human heart failure. Naunyn Schmiedebergs Arch Pharmacol 377, 231–243 [PubMed: 18392808]

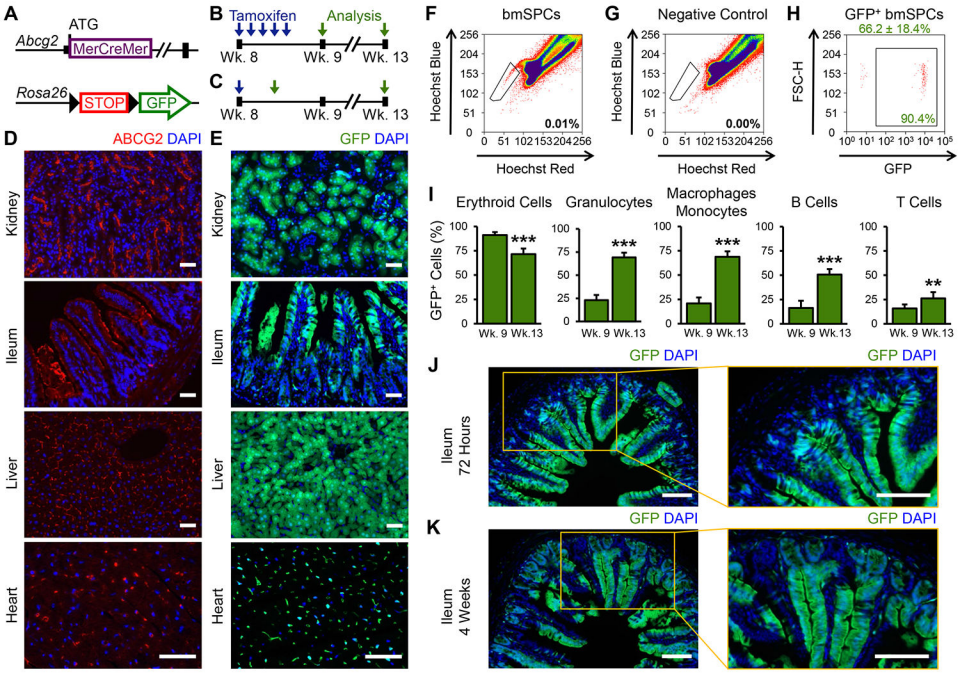


**Figure 1.**

Bone marrow SPCs and intestinal stem cells give rise to differentiated lineages *in vivo*. A) Genetics of experimental Abcg2$^{MCM/+}$ R26$^{GFP/+}$ mice. B) Experimental timeline used to evaluate GFP-labeling in bone marrow and cardiac studies 72 hours and four weeks (green arrows) after five consecutive daily 2 mg tamoxifen injections (blue arrows). C) Experimental timeline used to induce recombination in intestinal studies. GFP-labeling was assessed 72 hours and four weeks after single 2 mg tamoxifen injections. D) Immunofluorescence images of sections from C57Bl/6J mice stained for ABCG2. E) Images of native GFP fluorescence of sections from tamoxifen-injected Abcg2$^{MCM/+}$ R26$^{GFP/+}$ mice at week 9. F) Flow cytometry plot of bone marrow SPCs (bmSPCs) in tamoxifen-injected Abcg2$^{MCM/+}$ R26$^{GFP/+}$ mice (bmSPCs within black gate, number within plot represents percent of bmSPCs for this sample). G) Corresponding flow cytometry plot of negative control stained with Verapamil (bmSPCs within black gate, number represents percent of bmSPCs for this sample). H) Flow cytometry plot of GFP fluorescence of bmSPCs (percent GFP$^+$ bmSPCs above plot, mean ± SD, n=6). I) Flow cytometric analysis of bone marrow lineages labeled with GFP at week 9 (n=6) and week 13 (n=6). J) Native GFP fluorescent images of ileal sections from Abcg2$^{MCM/+}$ R26$^{GFP/+}$ mice 72 hours after a single tamoxifen injection with higher magnification image to the right. (K) Native GFP fluorescent images of ileal sections from Abcg2$^{MCM/+}$ R26$^{GFP/+}$ mice four weeks after a single tamoxifen injection with higher magnification image to the right. Scale bars: 50 μm; Statistical significance obtained by student's t-test; ** $P < 0.01$ and *** $P < 0.001$.

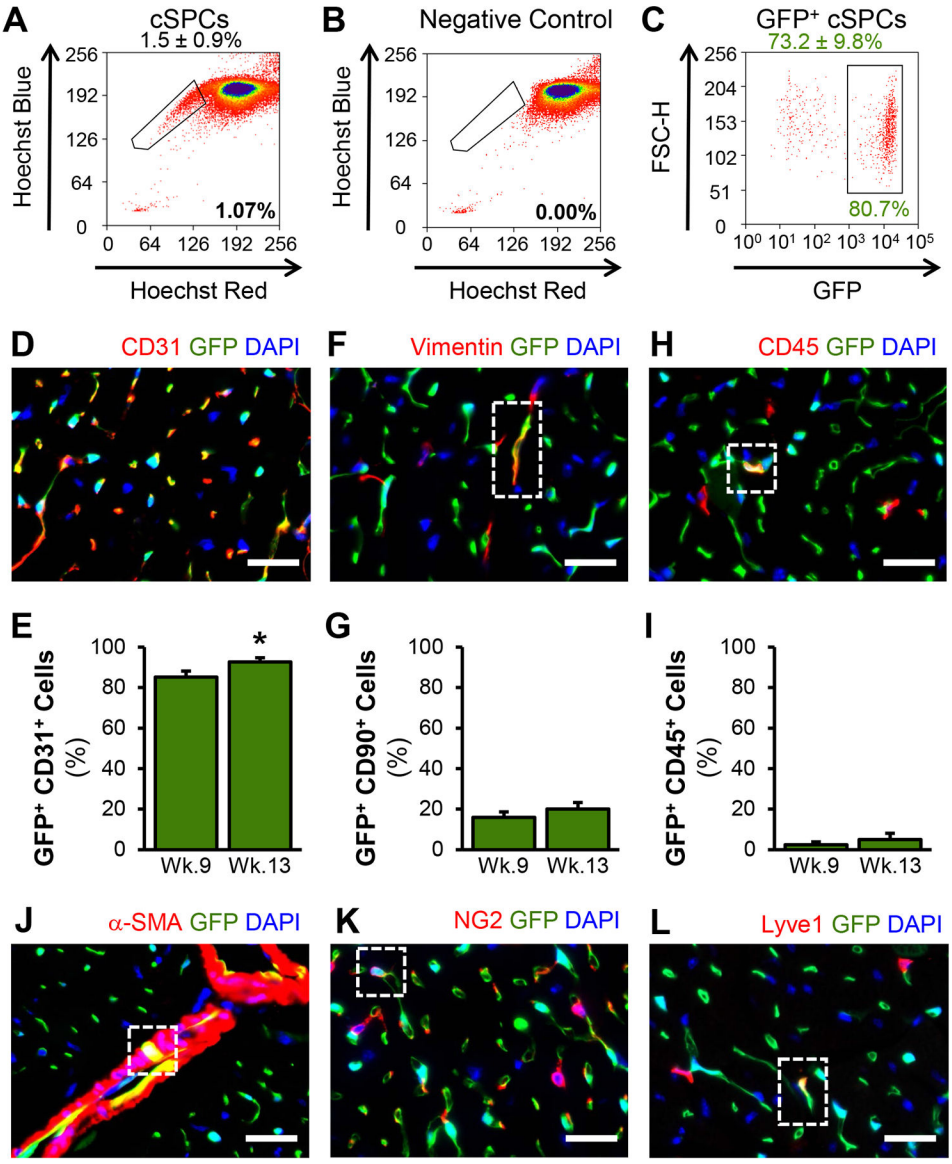


**Figure 2.**

Labeling of cSPCs and non-cardiomyocytes *in vivo* in the uninjured heart. A) Flow cytometry plot of cSPCs in Abcg2$^{MCM/+}$ R26$^{GFP/+}$ mice treated with tamoxifen (cSPCs within black gate, number inside plot is the percent of cSPCs for this sample, number above plot is mean ± SD, n=7). B) Corresponding flow cytometry plot of negative control cSPCs stained with Verapamil. C) Flow cytometry plot of GFP fluorescence of cSPCs (number within plot is the percent of GFP$^+$ cSPCs for this sample, number above plot is the mean ± SD, n=7). D) Immunofluorescence image of CD31 staining on cardiac sections from tamoxifen-injected Abcg2$^{MCM/+}$ R26$^{GFP/+}$ mice. E) Flow cytometry analysis of the percent of CD31$^+$ non-cardiomyocytes labeled with GFP at week 9 and week 13 (mean ± SD, n=4). F) Immunofluorescence image of Vimentin staining. G) Flow cytometry analysis of the percent of CD90$^+$ non-cardiomyocytes labeled with GFP at week 9 and week 13 (mean ± SD, n=4). H) Immunofluorescence image of CD45 staining. I) Flow cytometry analysis of

the percent of $CD45^+$ non-cardiomyocytes labeled with GFP at week 9 and week 13 (mean ± SD, n=4). J) Immunofluorescence image of alpha-smooth muscle actin. K) Immunofluorescence image of NG2 chondroitin sulfate proteoglycan staining. L) Immunofluorescence image of Lyve1 staining. Scale bars: 50 μm; Statistical significance was obtained by student's t-test; * $P < 0.05$.

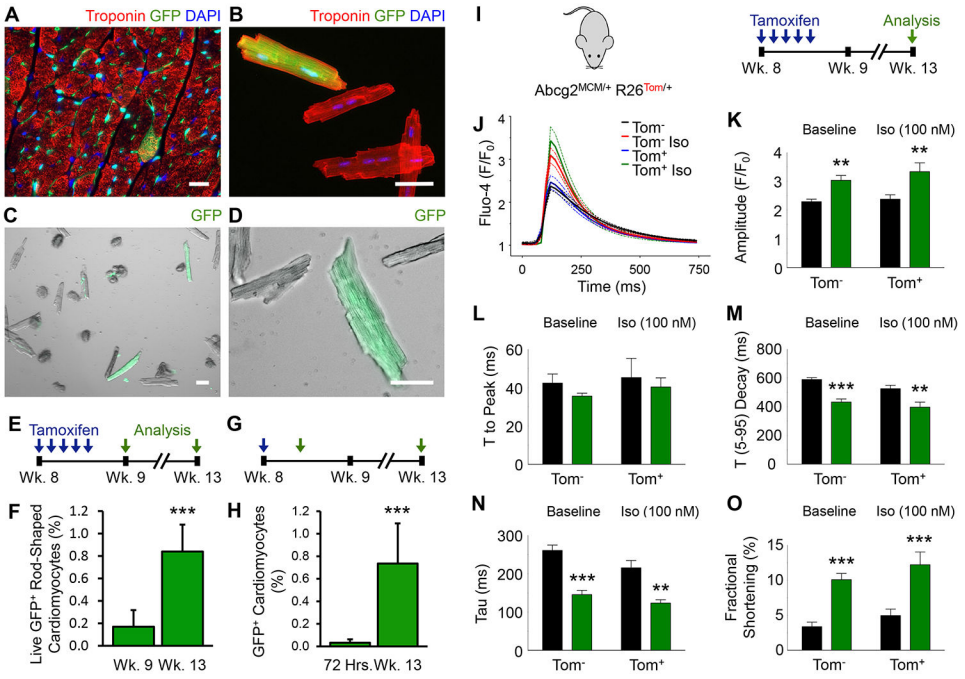


**Figure 3.**

CSPCs give rise to cardiomyocytes *in vivo* in the uninjured heart. A) Immunofluorescence image of Troponin I staining and native fluorescence of GFP on cardiac sections from tamoxifen-injected Abcg2$^{MCM/+}$ R26$^{GFP/+}$ mice. B) Immunofluorescence image of Troponin T staining and native GFP fluorescence of fixed, isolated adult cardiomyocytes. C) Image of native GFP fluorescence of live, isolated adult cardiomyocytes used to quantify GFP-labeling in tamoxifen-injected Abcg2$^{MCM/+}$ R26$^{GFP/+}$ mice. D) Higher-magnification image of GFP-labeled cardiomyocyte. E) Experimental timeline used to evaluate cardiomyocyte GFP-labeling 72 hours and four weeks (green arrows) after five consecutive daily 2 mg tamoxifen injections (blue arrows). F) Quantification of GFP-expressing cardiomyocytes as a percent of total live, rod-shaped cardiomyocytes at week 9 (n=5) and week 13 (n=7). G) Experimental timeline used to evaluate cardiomyocyte GFP-labeling 72-hours and 4 weeks following single 2 mg tamoxifen injection. H) Quantification of GFP-expressing cardiomyocytes at 72 hours (n=5) and 4 weeks (n=6) following a single 2 mg tamoxifen injection. I) Experimental timeline used for calcium dynamics measurements in Abcg2$^{MCM/+}$ R26$^{Tom/+}$ mice. J) Representative Fluo-4 traces of individual Tomato$^{-}$ and Tomato$^{+}$ cardiomyocytes with and without isoproterenol stimulation (Iso 100nM). K) Amplitude of pacing-induced cytosolic calcium traces (1Hz). L) Time (T) to peak Fluo-4 fluorescence of pacing-induced cytosolic calcium traces. M) Time from 5% to 95% of decay of Fluo-4 fluorescence of pacing-induced cytosolic calcium traces. N) Time constant of $Ca^{2+}$ transient decay (Tau) of pacing-induced cytosolic calcium traces. O) Fractional shortening of cardiomyocytes. Scale bars: 50 μm. Statistical significance was obtained by student's t-test to compare two groups and 2-way ANOVA to compare multiple groups; * $P < 0.05$, ** $P < 0.01$, *** $P < 0.001$.

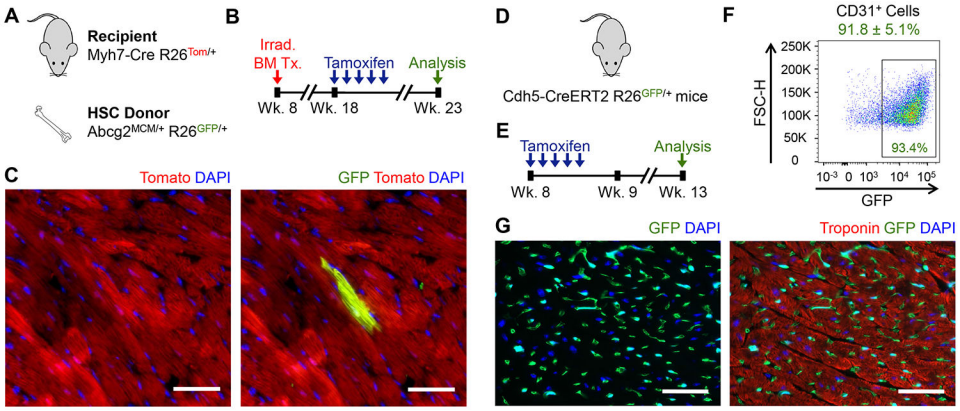


**Figure 4.**

Labeled bone marrow and endothelial cells do not contribute to lineage-traced cardiomyocytes. A) Bone marrow donor and recipient mice used to generate chimeric Myh7-Cre R26$^{tdTomato/+}$ mice with Abcg2$^{MCM/+}$ R26$^{GFP/+}$ bone marrow. B) Experimental timeline for bone marrow chimera experiments. C) Representative fluorescent image of GFP$^{+}$ and Tom$^{+}$ cardiomyocytes in bone marrow chimeric mice four weeks after the fifth tamoxifen injection. D) BAC-Cdh5-CreERT2 R26$^{GFP/+}$ mice used to evaluate endothelial cell contribution to cardiomyocyte lineage-tracing. E) Experimental timeline for endothelial cell studies. F) Flow cytometry plot of GFP-expression in CD31$^{+}$ non-cardiomyocytes at week 13 (number within gate is percent of CD31+ non-cardiomyocytes that express GFP for this representative sample, number above is mean ± SD, n=4). G) Fluorescent image of Troponin I staining and native GFP fluorescence at week 13 (n=5). Scale bars: 50 μm.

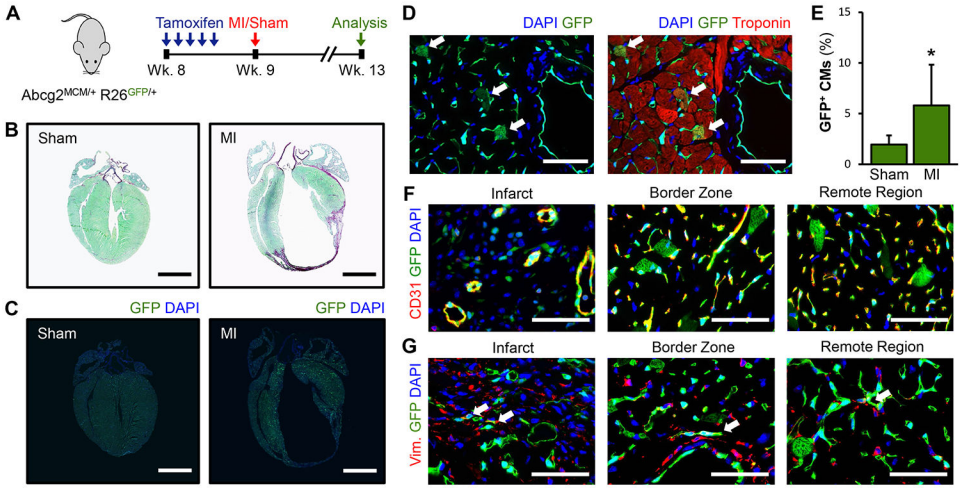


**Figure 5.**

Myocardial ischemic (MI) injury increases lineage-traced cardiomyocytes. A) Experimental timeline used to evaluate lineage-tracing of cardiomyocytes following MI in Abcg2$^{MCM/+}$ R26$^{GFP/+}$ mice. Seventy-two hours after the final tamoxifen injections were given, MI or sham operations were performed. Cardiomyocyte labeling was assessed 72 hours and 4 weeks later. B) Brightfield images of Sirius Red Fast Green stained cardiac sections from sham and MI-operated Abcg2$^{MCM/+}$ R26$^{GFP/+}$ mice at week 13. C) Images of native GFP fluorescence of cardiac sections from sham and MI-operated Abcg2$^{MCM/+}$ R26$^{GFP/+}$ mice. D) Fluorescence images of Troponin I staining and native GFP fluorescence of cardiac sections from an MI-operated Abcg2$^{MCM/+}$ R26$^{GFP/+}$ mouse. E) Quantification of cardiomyocytes expressing GFP (white arrows) on cardiac sections from sham-operated (n=7) and MI-operated (n=8) Abcg2$^{MCM/+}$ R26$^{GFP/+}$ mice (mean ± SD). F) Immunofluorescence images of CD31 staining in Abcg2$^{MCM/+}$ R26$^{GFP/+}$ mice four weeks following MI. G) Immunofluorescence images of Vimentin staining. White arrows highlight cells that express both GFP and Vimentin. Scale bars: 2 mm (B and C) and 50 μm (D, F and G). Statistical significance was obtained by student's t-test; * $P < 0.05$.

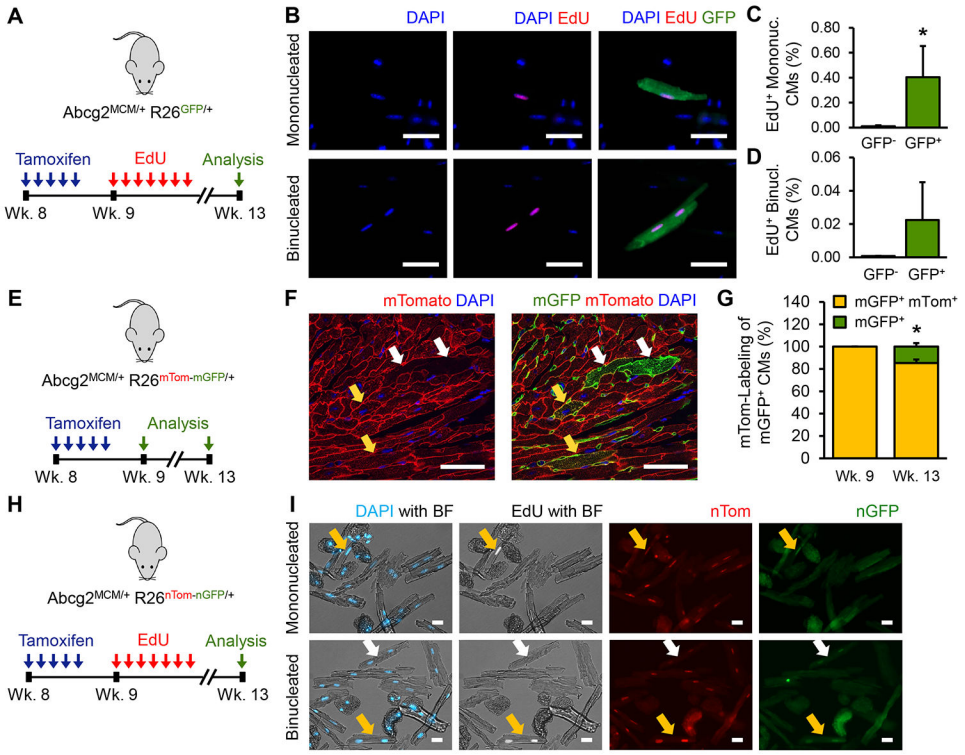


**Figure 6.**

Cardiac SPCs fuse with preexisting cardiomyocytes to stimulate cardiomyocyte proliferation. A) Experimental design to assess cardiomyocyte cell cycle activation in lineage-traced cardiomyocytes. B) Fluorescent images of mononucleated and binucleated $EdU^+$ $GFP^+$ isolated adult cardiomyocytes from $Abcg2^{MCM/+}$ $R26^{GFP/+}$ mice. C) Quantification of the percent of $GFP^-$ and $GFP^+$ mononucleated, rod-shaped cardiomyocytes that are $EdU^+$ at week 13 (mean ± SD, n=4). D) Quantification of the percent of $GFP^-$ and $GFP^+$ binucleated, rod-shaped cardiomyocytes that are $EdU^+$ at week 13 (mean ± SD, n=4). E) Experimental design to assess cellular fusion in $Abcg2^{MCM/+}$ $R26^{mTom\text{-}mGFP/+}$ mice. F) Fluorescent image of $mGFP^+$ $mTom^+$ cardiomyocytes (yellow arrows) and $mGFP^+$ cardiomyocytes (white arrows). G) Quantification of the percentage of $mGFP^+$ cardiomyocytes that are $mTom^+$ (yellow) or $mTom^-$ (green) at week 9 (n=5) and week 13 (mean ± SD, n=4). H) Experimental design to assess the role of cellular fusion in proliferative lineage-traced cardiomyocytes. I) Fluorescent images of mononucleated and binucleated $EdU^+$ $nGFP^+$ isolated adult cardiomyocytes that are $nTom^+$ (yellow arrow) or $nTom^-$ (white arrow) from $Abcg2^{MCM/+}$ $R26^{nTom\text{-}nGFP/+}$ mice. Scale bars: 25 μm. Statistical significance was obtained by student's t-test; * $P < 0.05$.

**Table 1.**

Labeling of bone marrow SPCs and differentiated lineages in chimeric Myh7-Cre $R26^{Tom/+}$ mice with $Abcg2^{MCM/+}$ $R26^{GFP/+}$ bone marrow.

| Bone Marrow Cell Type | $GFP^+$ Cells (%) |
|---|---|
| Side Population Cells | 40.5 ± 9.30 |
| LSK ($Lin^-$ $Sca\text{-}1^+$ $Kit^+$) | 56.9 ± 7.31 |
| Granulocytes (Ly-6C and Ly-6G/Gr-1) | 56.9 ± 7.23 |
| Monocytes/Macrophages (CD11b/Mac-1) | 58.0 ± 7.50 |
| Erythroid Cells (Ter-119) | 50.4 ± 6.80 |
| B Cells (CD45R/B220) | 40.1 ± 6.30 |
| T Cells (CD3ε) | 14.0 ± 3.00 |

Percentages are mean ± standard deviation (n=5).